**Atmospheric
Chemistry
and Physics
Discussions**

Variability of aerosol vertical distribution in the Sahel

O. Cavalieri[1], F. Cairo[1], F. Fierli[1], G. Di Donfrancesco[2], M. Snels[1], M. Viterbini[1],
F. Cardillo[1], B. Chatenet[3], P. Formenti[3], B. Marticorena[3], and J. L. Rajot[4]

[1]Consiglio Nazionale delle Ricerche-Istituto di Scienze dell'Atmosfera e del Clima, Rome, Italy
[2]Ente per le Nuove Tecnologie Energia e Ambiente, Frascati, Italy
[3]LISA, Universités Paris Est-Paris Diderot-Paris 7, CNRS, Créteil, France
[4]IRD-UMR 211 Bioemco, Niamey, Niger

Correspondence to: F. Cairo (francesco.cairo@artov.isac.cnr.it)

ACPD

10, 17609–17655, 2010

**Variability of aerosol
vertical distribution
in the Sahel**

O. Cavalieri et al.

Full Screen / Esc

Printer-friendly Version

Interactive Discussion

**Variability of aerosol
vertical distribution
in the Sahel**

O. Cavalieri et al.

Full Screen / Esc

Printer-friendly Version

Interactive Discussion

Abstract

We present and discuss ground-based and satellite observations of aerosol optical properties over Sahelian Africa for the years 2006, 2007 and 2008.

This study combines data acquired by three ground-based micro lidar systems located in Banizoumbou (Niger), Cinzana (Mali) and M'Bour (Senegal) in the framework of the African Monsoon Multidisciplinary Analysis (AMMA), by the AEROsol RObotic NETwork (AERONET) sun-photometers and by the space-based Cloud-Aerosol Lidar with Orthogonal Polarization (CALIOP) onboard Cloud-Aerosol Lidar and Infrared Pathfinder Satellite Observations (CALIPSO).

The 2006 seasonal pattern of the aerosols vertical distribution is presented. It shows the presence of aerosol mainly confined in the lower levels of the atmosphere during the dry season, with the aerosol layer increasing in vertical extension and absolute values in spring, reaching the largest values in summer in correspondence with a progressive clearing up of the atmosphere at the lowermost levels.

Aerosol produced by biomass burning are observed mainly during the dry season, when north-easterly air masses pass over large biomass burning areas before recirculating over the measurement sites. This kind of aerosol is present mainly in layers between 2 and 6 km of altitude, although episodically it may show also below 2 km, as observed in Banizoumbou (Niger) in 2006. Biomass burning aerosol is also observed during spring when air masses originating from North and East Africa pass over sparse biomass burning sources, and during summer when biomass burning aerosol is transported from the southern part of the continent by the monsoon flow.

The summer season on the whole is characterized by a large presence of desert dust along the entire Sahelian region, widespread in altitude with Aerosol Optical Depths above 0.2.

The interannual variability in the three year monitoring period is not very significant. An analysis of the aerosol transport pathways, aiming at detecting the main source regions, revealed that air originated from the Saharan desert is present all year long

Full Screen / Esc

Printer-friendly Version

Interactive Discussion

and it is observed in the lower levels of the atmosphere at the beginning and at the end of the year. In the central part of the year it extends upward and the lower levels are less affected by air masses from Saharan desert when the monsoon flow carries inland air from the Guinea Gulf and Southern Hemisphere. Biomass burning is mainly
5 confined in the higher layers and observable in winter and in autumn.

1 Introduction

Africa is the world's largest source of biomass burning aerosol (BBA) and desert dust (DD), which constitute the majority of aerosol present in the Sahelian region (Prospero et al., 2002). Satellite imagery shows frequent and vast plumes of dust and smoke
10 emerging from Africa and spanning the entire Tropical Atlantic and Mediterranean region.

Both dust and biomass burning aerosol influences the Earth's radiative budget by scattering and absorbing solar radiation (Haywood and Boucher, 2001; Eck et al., 2003; Magi et al., 2003; Haywood et al., 2003) while dust particles are sufficiently large to
15 interact directly with terrestrial radiation as well (Foster et al., 2007).

The pattern of aerosol emissions, particularly biomass burning smoke, over West Africa follows a well determined seasonal cycle related to the seasonal shift of the Inter-Tropical Convergence Zone (ITCZ) which moves northward and crosses 15° N by the end of June and retreats southward again in September. Maximum emissions
20 of biomass burning aerosol from the regions of northern Africa occur during the dry season from December to February with very little open biomass burning occurring during August-November (Haywood et al., 2008).

Far from the sources, dust or biomass burning aerosols are frequently observed in elevated layers (Prospero et Carlson, 1972; Ansmann et al., 2003).
25 Dust storms occur throughout the whole year, peaking in springtime (Marticorena and Bergametti, 1996) while westward transport over Atlantic Ocean peaks during the summer as a result of large-scale dust outbreaks is mostly confined to a deep mixed

layer (the Saharan Air Layer) (Leon et al., 2009; Prospero et Carlson, 1972). Much of these dust aerosols are transported westward under the influence of the trade winds while northward transport toward the Mediterranean is linked to the presence of cyclones (Moulin et al., 1997; Alpert et al., 1990; Dayan et al., 1991). The zone of maximum dust transport shift from ∼5° N during winter to ∼20° N during summer and it is associated with the latitudinal movement of the large-scale circulation, including that of the Intertropical Convergence Zone (Moulin et al., 1997).

Long term aerosol studies have shown a seasonal pattern of the transport of African dust: during winter, the desert aerosols are transported across the Atlantic towards the north-eastern cost of South America (Swap et al., 1992) while during summer dust is transported more northward above the trade winds atmospheric layer and extends as far as the Caribbean sea and the south-eastern United States (Prospero and Carlson, 1972).

Several field campaigns have been conducted in Africa to study atmospheric particles and their optical properties and to understand the influence of these two types of aerosol on the regional climate.

A classification of the physical and optical properties of mineral dust aerosols emitted from the African continent has been performed in the frame of the Saharan Dust Experiment (SHADE) that took place in late September 2000 (Tanrè et al., 2003).

Similarly, biomass burning aerosols emitted from South Africa were studied during Southern African Regional Science Initiative (SAFARI) field campaign conducted during the August–September 2000 dry season (Schmid et al., 2003; Magi et al., 2003; Haywood et al., 2003; Swap et al., 2003).

Recently, the African Monsoon Multidisciplinary Analysis (AMMA) project performed extensive multiannual series of observations in Sahelian Africa. AMMA is an international project with the goal to improve the knowledge and the understanding of the Western African Monsoon, its variability on daily to inter-annual timescales and its influence on the physical, chemical and biological environment on a regional and global scale. AMMA involved three observation periods: the long term observation period

Variability of aerosol vertical distribution in the Sahel

O. Cavalieri et al.

(LOP) concerned with historical observations and additional long term observations (2001–2010) to study the inter-annual to decadal variability, the enhanced observation period (EOP) planned to serve as a link between LOP and more focused observations, during special observation periods (SOP). The EOP main objective was to document the annual cycle of the surface and atmospheric conditions over a climatic transect and to study the surface memory effects at the seasonal scale, over three years (2005–2007).

The SOP periods took place in the West African Sahel in 2006 and focused on detailed observation of specific processes and weather systems during the dry season (SOP0, January–February) and at various key stages of the rainy season during three periods in summer 2006: the monsoon onset (SOP1, 15 May–30 June), the peak monsoon (SOP2, 1 July–14 August) and finally the late monsoon (SOP3, 15 August–15 September) (Redelsperger, 2006).

The identification and characterization of aerosol sources and the study of the evolution and the effects of atmospheric aerosols were among the objectives of the AMMA effort. In its framework, several studies focussing on aerosol have thus been performed.

Ground-based measurements of aerosol mass, optical properties and vertical distribution over M'Bour (Senegal) from 2006 to 2008 have been reported by Leon et al. (2009) showing that the maximum in the dust activity was observed in summer (June–July) corresponding to a maximum in the aerosol optical thickness and single scattering albedo, although severe dust storms were also observed in spring (March). Sporadic events of biomass burning aerosols were observed in winter, particularly in January 2006.

Haywood et al. (2008), investigated tropospheric aerosol transport over West Africa and the associated meteorological conditions during the dry season, combining data from ultra-light aircraft borne-lidar, airborne in situ aerosol and gas measurements, satellite based aerosol measurements, air mass trajectories and radiosonde measurements.

High concentrations of mineral dust aerosol were typically observed from the surface

up to 1.5 or 2 km associated with Saharan air masses. At higher altitudes concentration of biomass burning aerosol were typically observed between 2–5 km of altitude (Johnson et al., 2008; Osborne et al., 2008; Raut et Chazette, 2008).

Heese and Wiegner (2008), reported lidar measurements of the vertical distribution of optical particle properties performed during January 2006 in Banizoumbou (Niger). The profiles show a varying dust layer in the planetary boundary layer during the whole period and a layer of biomass burning aerosol from the PBL up to an altitude of 5 km was frequently observed.

The objective of this paper is twofold: 1) to study the seasonal and inter-annual variability of aerosol optical properties and the aerosol vertical distribution in the Sahelian region over three years and 2) to characterize the different kind of aerosols present in the atmosphere and observed by lidar in relation to the origin of the air masses arriving in the Sahel area.

The study of the inter-seasonal aerosol vertical distribution variability was conducted on the basis of the dataset collected in 2006 by three micro lidar systems (MULIDs) deployed in M'Bour (Senegal), Cinzana (Mali) and Banizoumbou (Niger), while to characterize the inter-annual variability of the aerosol vertical profiles, we analyzed the space-based lidar observations from CALIOP for the years 2006, 2007 and 2008.

In order to characterize the different kind of aerosols present in the atmosphere, we have also used aerosol optical thickness and Angstrom coefficient data obtained by sun-photometers located at three AEROsol RObotic NETwork (AERONET) stations. 3-years back-trajectories are analyzed to identify the origin of the airmasses sampled by ground based and satellite lidars and biomass burning sources location and variability have been identified with fire products from the ATSR World Fire Atlas.

The paper is organized as follows: in Sect. 2 the optical parameters observed by different instruments are defined and discussed. Section 3 provides the analysis of aerosol seasonal patterns from MULID observations performed in Niger, Mali and Senegal sites in 2006. Section 4 presents the study of the aerosol inter-annual and intra-annual variability using measurements from the satellite lidar CALIOP over 2006,

2007 and 2008. Section 5 depicts a general aerosol climatology and tries to link it to the general circulation patterns in the Sahel. Section 6 draws the conclusions of our study.

2   Instrumentation and methods

2.1   Optical properties

The elastic lidar technique is a robust system to retrieve the vertical profile of aerosol optical properties (Di Donfrancesco et al., 2006; Di Sarra et al., 2001; Gobbi et al., 2000). The parameter directly accessible is the attenuated backscattering coefficient $S(z)$, whose range corrected and energy normalized, equation is given by :

$$S(z) = K\beta(z)\exp\left(-2\int_0^z \alpha(x)\,dx\right) \qquad (1)$$

where z is the altitude/range, α and β are respectively the extinction and backscattering coefficients, and K is a constant.

The backscattering and extinction coefficients α and β have contributions from both molecules and aerosol.

$$\alpha(z) = \alpha_a(z) + \alpha_m(z)$$
$$\beta(z) = \beta_a(z) + \beta_m(z) \qquad (2)$$

The backscatter ratio R is defined as the ratio between the total backscattered radiation and the molecular backscatter:

$$R = (\beta_m + \beta_a)/\beta_m \qquad (3)$$

Variability of aerosol vertical distribution in the Sahel

O. Cavalieri et al.

O. Cavalieri et al.

where β_m is the molecular backscatter and β_a is the aerosol backscatter. $(\beta_m + \beta_a)$ is proportional to the lidar signal while β_m is calculated (say how you calculate it. For instance Raman lidar can calculate it directly from lidar signal) from ancillary data, as radio sounding density profiles or atmospheric models.

5   The lidar ratio is defined as:

$$L_a(z) = \frac{\alpha_a(z)}{\beta_a(z)} \text{ and } L_m(z) = \frac{8\pi}{3} \tag{4}$$

While L_m is given by light scattering theory, The aerosol lidar ratio L_a can vary widely depending on the aerosol size distribution, refractive index and shape. Typical values of the aerosol lidar ratio are below 30 sr for maritime aerosols, from 30 to 50 sr for mineral

10 dust and around 60–70 sr for biomass burning aerosols. Both aerosol backscatter and extinction coefficient are variables in Eq. (1) lidar ratio is assumed to invert the lidar equation.

Although it is often assumed to use prescribed values for the aerosol lidar ratio, based on the kind of aerosol one expects, one might also vary this parameter in order

15 to get a better agreement with other optical parameters obtained by co-located measurements of other optical instruments. The inversion applied here uses a variable lidar ratio that is selected, or each lidar profile, in order to best fit with co-located Aerosol Optical Depth measurements taken by an AERONET sunphotometer. A detailed description of the method and the application to selected observation in Banizoumbou is

20 reported in Cavalieri et al. (2010).

The Volume Depolarization Ratio D, is defined as the ratio between the parallel $(\beta^{//})$ and perpendicular $(\beta^{\perp})$ polarization components.:

$$D = \frac{\beta^{\perp}}{\beta^{//}} \tag{5}$$

Apart from a known contribution from the air molecules, D has a variable contribution

25 from the suspended aerosols and clouds, depending on the number, shape and size of the particles.

D provides an indication of the particle shape and, to a lesser extent, of their size, because only non-spherical particles can produce a change in the polarization plane of the backscattered light (Reagan et al., 1989). Thus it allows to distinguish between spherical, small non spherical (i.e. biomass burning aerosol) and large non-spherical particles (i.e. mineral dust) (Mishenko et al., 1997). Values close to zero are expected for spherical particles, and higher values are produced by non spherical particles.

In our analysis, we have used R and D to discriminate between biomass and dust aerosol (Balis et al., 2004; Heese and Wiegner, 2009). Dust is characterized by higher lidar ratio with values from 30 to 50 sr and volume depolarization greater than 10% (see for instance Mona et al., 2006; De Tomasi et al., 2003; Tafuro et al., 2003; Mattis et al., 2002b; Immler and Schrems, 2006; Cattrall et al., 2005) while BBA by lidar ratio value $\sim$ 60–70 sr and volume depolarization often lower than 10% (Balis et al., 2003; Wandinger et al., 2002; Cattrall et al., 2005; Ferrare et al., 2001; Fiebig et al., 2002).

The microphysical properties of aerosols are strongly correlated to the wavelength dependence of the extinction and backscatter coefficient. For the latter, such dependence is expressed in terms of the color index $C(z)$ expressed as:

$$C(z) = \frac{-\ln\left(\beta_a^{\lambda_1}(z)/\beta_a^{\lambda_2}(z)\right)}{\ln\left(\lambda_1/\lambda_2\right)} \tag{6}$$

where $\beta_a^{\lambda 1}$ and $\beta_a^{\lambda 2}$ represents the aerosol backscatter coefficient at wavelengths λ_1 and λ_2.

In this work λ_1 is equal to 532 nm and λ_2 to 1064 nm so positive $C(z)$ indicates that aerosol backscatter decreases with increasing wavelength. Color index is used to retrieve qualitative information about the size of scatteres since large $C(z)$ indicates the abundance of particles with radii smaller than the lidar wavelengths, whereas smaller $C(z)$ indicates the predominance of large particles (Liu and Mishenko, 2001).

On the other hand, color index can be used to identify dust aerosol since their wavelength dependence of the absorption properties causes $C(z)$ to become strongly negative while it remains around 0 for a non-absorbing aerosol (Immler and Schrems, 2003).

Title Page

Abstract | Introduction

Conclusions | References

Tables | Figures

◄ | ►

◄ | ►

Back | Close

Full Screen / Esc

Printer-friendly Version

Interactive Discussion

$C(z)$ close to 0, as encountered in low level clouds, indicates the presence of particles much larger than the LIDAR wavelength. Based on these properties color index has been used here as a tool to discriminate biomass burning aerosol from dust, the latter being generally larger in size (>1 μm). The color index is typically below 0.5 for large dust particles (Ansmann et al., 2003) and in particular even smaller values for Saharan dust, while greater values indicate the presence of smaller particles (<1 μm) (Balis et al., 2004; Rajot et al., 2008).

In order to quantify the overall aerosol abundance in the air column from lidar profile and to compare it with integrated observations such as, the aerosol optical depth (AOD) has been used. This is defined as the integrated aerosol extinction coefficient over a vertical column of unit cross section:

$$AOD = \int_0^\infty \alpha_{aer}(z)dz \tag{7}$$

and can be retrieved both from lidar measurements, integrating the extinction over the profile, and from sunphotometric observations (Devara et al., 1996). The AOD directly depends on the total aerosol mass, although it also depends on the size and refractive index of the particles. Similarly to the case of the spectral dependence of the backscatter coefficient, the wavelength, the AOD, and the atmospheric turbidity (haziness) are related through the Angstrom's turbidity formula:

$$AOD = B\lambda^{-A} \tag{8}$$

where B is the Angstrom turbidity coefficient, λ is the wavelength in microns, and A is the Angstrom exponent. A and B are independent from wavelength, and can be used to describe the size distribution of aerosol particles and the general haziness of the atmosphere. For two different wavelengths,

$$AOD_1 = B\lambda_1^{-A}$$

$$AOD_2 = B\lambda_2^{-A} \tag{9}$$

from which the Angstrom coefficient A, can be retrieved.

$$A = \frac{\ln\left(AOD_1/AOD_2\right)}{\ln\left(\lambda_2/\lambda_1\right)} \tag{10}$$

Larger values of A implies a relatively high ratio of small to large ($r > 0.5\,\mu m$) while when larger particles dominate the distribution A gets smaller. As a result, small aerosol particles such as biomass burning aerosols interact more strongly with the shorter wavelengths of solar spectrum while mineral dust particles interact with all solar spectrum approximately equally. Consequently, for biomass burning aerosol A assumes values between 1 and 1.5 while for mineral dust it is typically close to zero (Johnson et al., 2008; Pelon et al., 2008). The mixing between these type of particles tend to change the Angstrom coefficient in the range 0–1.5 (Hamonou et al., 1999).

A synopsis of the criteria used to classify the main types of aerosol from the above mentioned optical coefficient is depicted in Table 1.

2.1.1 Mulid lidars

Three micro lidar (MULID) have been deployed along a longitudinal transect named in the Sahelian region, where transport from the dust source regions toward West occur, in M'Bour (Senegal, 14.23° N–16.57° W), Cinzana (Mali, 13.16° N–5.56° W) and Banizoumbou (Niger, 13.5° N–2.6° E) .

The MULID systems are newly developed portable low power consumption lidars adapted for a field use in a semiautomatic mode in remote sites powered only by solar panels.

The main optical and electronic MULID characteristics are listed in Table 2.

In Cinzana the lidar was located out site, close to a small building (scientific offices) of the Agronomical Research station of Cinzana, at about 2 m above the ground while in M'Bour station it was positioned on the roof of a building at 10 m from the ground. Cinzana is a rural stations, surrounded by open fields; the measurement station is

Variability of aerosol vertical distribution in the Sahel

O. Cavalieri et al.

Title Page

Abstract | Introduction

Conclusions | References

Tables | Figures

◄ | ►

◄ | ►

Back | Close

Full Screen / Esc

Printer-friendly Version

Interactive Discussion

hosted by the "Station de Reserche Agronomique de Cinzana" depending on the "Institut d'economie Rurale" of Mali. In M'Bour, the lidar is installed at the "Station de geophysique" of the Institut de Reserche pour le Developpment", inside a protected natural area, facing the Atlantic Ocean, south of the city of M'Bour (180 000–200 000 inhabitants). Along with the lidar systems, the sites hosted a sunphotometer of Aeronet. The M'Bour site being one of the three super-sites implemented in Africa for the AMMA activities, was also equipped with particle counters, nephelometers and aethalometers for the SOP0 and with fluximeters all along the EOP.

The station in Banizoumbou hosted the MULID in a small hut. The station is located in the countryside at a distance of 60 km east from the capital of Niger, Niamey, and was a second super site for the AMMA project, hosting instruments for a complete characterization of the aerosol properties. This site has been operational since the early nineties, when the first measurements of soil erosion were performed on a cultivated field and a fallow (Balis et al., 2004; Rajot, 2001).A sunphotometer station AERONET is implemented close to Banizoumbou since 1995.

For the complete list and description of instruments placed in the Banizoumbou and M'Bour super sites the reader may refer to: http://amma.mediasfrance.org/implementation/instruments/.

Details on the instrumental set-up and date inversion algorithm are given in O. Cavalieri et al. (2010) here only a brief account will be given.

Let $S'(z)$ be the range corrected and background subtracted signal, the total attenuated backscattering ratio R' defined as $R'(z) = K_R S'(z)/\beta_m$ was obtained by iteratively correcting R' for cloud, aerosol and molecular attenuation until the process converged to a stable value R. The coefficient K_R has been chosen to impose $R'(z) = 1$ in a region of the atmosphere supposedly free of aerosols and the molecular profile is adopted as a reference profile for the free portion $S'(z)$.

The MULIDs have been installed at the end of January 2006 and have provided daily observations for 2006 except for some periods were not covered by measurements due to problems with the laser heads. Daily backscatter and depolarization

Variability of aerosol vertical distribution in the Sahel

O. Cavalieri et al.

Title Page

Abstract | Introduction

Conclusions | References

Tables | Figures

◄ | ►◄

◄ | ►

Back | Close

Full Screen / Esc

Printer-friendly Version

Interactive Discussion

profiles with 30 m vertical resolution are available. Two measurement sessions per day, at fixed hours in the morning and in the evening, each session lasting 1 h, were performed. During SOPs, additional measurement sessions were performed often in coincidence with other campaign activities, such as aircraft overpasses to provide full daily coverage.

AOD was retrieved integrating the extinction profile from the bottom to the top of the sounding.

2.1.2 CALIOP lidar

The CALIPSO satellite hosts the CALIOP elastic backscattering lidar that provides information on the vertical distribution of aerosols and clouds as well as on their optical and physical properties over the globe with unprecedented spatial resolution (Winker et al., 2007). Linearly polarized laser pulses are transmitted at 532 nm and 1064 nm. The 1064 nm receiver channel is polarization insensitive, while the two 532 nm channels separately measure the components of the 532 nm backscatter signal polarized parallel and perpendicular to the outgoing beam.

Observations of total and perpendicular attenuated backscattering intensity at 532 nm and total attenuated backscattering intensity at 1064 are available on http://eosweb.larc.nasa.gov/HBDOCS/langley_web_tool.html and analyzed in this study. The vertical resolution is 30 m and 60 m and the horizontal resolution 333 m and 1 km for altitudes between −0.5 km and 8.2 km and between 8.2 and 20.2 km, respectively. The backscatter coefficient profiles were derived from the calibrated, range corrected, laser energy normalized, background noise subtracted lidar return signal (Winker et al., 2007; Kim et al., 2008). The depolarization ratio is calculated with Eq. (5) as the ratio between perpendicular and parallel polarized backscatter signal at 532 nm and the color ratio is calculated with Eq. (5) with λ_1=532 nm and λ_2=1064 nm For our study, for comparison with the data provided by the ground based stations, we have grouped the CALIOP measurements acquired in the latitudinal band 11° N–15° N into three sub-sets at different longitude (i) 0° E–5° E, (ii) 5° W–10° W, (iii) 15° W–20° W. These regions cov-

ered the Sahelian transect, each one containing at its centre one of the three ground based stations where the MULID were hosted. For each satellite orbit, a single vertical profile has been created by averaging the nearest 20 CALIOP profiles to the selected locations. These profiles were smoothed in the vertical at intervals of 300 m from the surface to 8.2 km.

The analysed dataset extends from 13 June 2006 to end of 2008. Satellite passage occurs at around 01:30 GMT and 13:00 GMT for Banizoumbou, 02:00 GMT and 13:30 GMT for Cinzana, 02:00 GMT and 14:30 GMT for M'Bour regions.

Further information on the Caliop instrumentation and its products can be found at: http://eosweb.larc.nasa.gov/PRODOCS/calipso/table_calipso.html.

2.1.3 AERONET sunphotometers

The field campaign activities have been supported by a network of passive radiometers which has been operative routinely in West Africa since 1995, within the activities of AERONET. This network of annual sky calibrated radiometers measures the direct solar radiance at eight wavelengths and sky radiance at four of these wavelengths, providing sufficient information to determine the aerosol size distribution and refractive index (Dubovik et al., 2000, 2002). This long-term, continuous and readily accessible database of aerosol optical, microphysical and radiative properties for aerosol research and characterization is available at http://aeronet.gsfc.nasa.gov/.

There, globally distributed observations of spectral aerosol optical depth (AOD) at 440, 675, 870 and 1020 nm and Angstrom coefficient A (the ratio of the AOD at two different wavelengths) data are available at three quality levels: level 1.0 (unscreened), level 1.5 (cloud-screened) and level 2.0 (cloud-screened and quality-assured). Almost daily data are available at the Banizoumbou, Cinzana and Dakar sites for the year 2006, 2007 and 2008 from about 07:00 a.m. to 05:00 p.m.

In this study, we used AOD data from level 2.0 and we interpolated the AOD data at 440 and 675 nm to obtain the equivalent AOD at 532 nm, the wavelength of lidar

Title Page

Abstract | Introduction

Conclusions | References

Tables | Figures

|◀ | ▶|

◀ | ▶

Back | Close

Full Screen / Esc

Printer-friendly Version

Interactive Discussion

measurements, by using the AOD spectral dependence (Angstrom, 1964) provided by:

$$\frac{AOD_{532}}{AOD_\lambda} = \left(\frac{532}{\lambda}\right)^{-A}$$

where the Angstrom exponent A is estimated with AOD at 440 and 675 nm.

2.2 Transport analysis

Air mass backtrajectories have been used to identify main circulation patterns in the region, and their seasonal variability. Trajectories, calculated 7 days backward at different altitudes above measurement sites, are retrieved from the http://aeronet.gsfc.nasa.gov/cgi-bin/bamgomas_interactive site, as a support for the AERONET program and for the BAMGOMAS (Back trajectories, Aeronet, Modis, Gocart, Mplnet Aerosol Synergism) project. The trajectories are based on a kinematic trajectories analysis using NASA GMAO (Global Modeling Assimilation Office) assimilated gridded analysis data (for 1 January 2000–30 August 2007) and from NCEP (National Centers for Environmental Prediction) analyses (31 August 2007 onward).

In order to identify biomass burning sources, the fire product ATSR World Fire Atlas is used to identify possible emission due to fires.

ATSR fire products are available from November 1995 to present on globally scale and monthly frequency.

We obtained data from the Advanced ATSR sensor onboard ENVISAT for year 2006, 2007 and 2008 from http://dup.esrin.esa.int/ionia/wfa/index.asp.

In order to identify dust and monsoon circulation patterns, air parcel positions are also matched with two regions representative of desert dust source and monsoon flow.

The region representative of desert dust source (called 'Desert' in section 5) is considered the area of Sahara Desert between 18°–30° N of latitude and 10° W–40° E of longitude while the region representative of monsoon flow is the area of the Guinea Gulf between 20° W–0° W of latitude and 10° W–20° E of longitude (called "Ocean" in Sect. 5).

3 Seasonal variability in 2006

144 profiles from February to August 2006 for the Niger site, 48 profiles from January to July 2006 for the Mali and 19 observations for the Senegal site are available. So it is possible to discuss the aerosol seasonal evolution during 2006 for Banizoumbou and Cinzana and, while for M'Bour the analysis is limited to the dry season in 2006 due to the limited time coverage.

A synopsis of the MULID measurements is presented in Fig. 1. The first panel (a) shows colour coded extinction profiles function of time (expressed in Julian Day) and altitude for Banizoumbou (left panel), Cinzana (central panel) and M'Bour (right panel) during 2006. Profiles extend up to 6 km and above that level we considered the aerosol contribution to the AOD to be negligible.

Second row (b) reports the aerosol mask which has been applied to highlight different kind of aerosols using extinction and depolarization values criterion to characterize different biomass and dust aerosol based on their different optical properties. Most of observations can be associated with a moderate dust load, with $D > 10\%$ and α laying in the range between 0.1 and 0.2 km^{-1}, and are not highlighted in these panels for sake of clarity. We have considered as intense dust events those with aerosols extinction coefficient values α larger than 0.2 km^{-1} and volume depolarization D larger than 10% (marked in red in Fig. 1b). We have considered as biomass burning aerosol observations those with α values between 0.05 and 0.2 and $D < 10\%$, which have been marked in green. Finally, observations characterized by higher extinction ($\alpha > 0.2$) and low depolarization ($D < 10\%$) values have been considered as events of mixing between dust and biomass aerosols and have been marked in blue in Fig. 1b.

Panels in row (c) show the altitude range where the AOD increases from 10% to 90% of its total value. The red triangles shows the altitude where AOD reaches its median value (50% of total) representative of the average altitude of the aerosol layers.

Finally, the panels in the row (d) report the integrated AOD.

In Banizoumbou, during the late dry season in February the aerosol content is gener-

ally low, with AOD between 0.1 and 0.2. Biomass burning are detected in the lowermost layers, tapering off with increasing altitude even if non negligible extinction values are observed up to 4 km. The aerosol burden increases at the beginning of the summer season and extends upward to 4–5 km altitude, mainly associated with moderate to
5 intense dust burdens with AOD around 0.1–0.4, although episodical biomass observations can be discerned, extending between 3 and 4 km. It is noteworthy that in general the aerosol tends to be present higher up in altitude and this is especially evident in May and June, when the lowermost layers are cleaner than in February. Remarkable are a few strong dust events lasting a few days around day 170 and 180 (end of May 2006),
10 with significant dust burdens at low level in the atmosphere, causing a net increase in AOD values, reaching values as high as 2.

From the database coverage it is difficult to infer when the transition between winter and summer regimes occurs.

A similar behaviour is observed in Cinzana, where in January the aerosol content is
15 generally larger than in Banizoumbou, with AOD around 0.15, and the aerosols (mainly biomass) between 1 and 5 km of altitude.

Biomass are observed more episodically in the summer season in the same range altitude while a mixture of the two kind of aerosols is often observed.

Large dust events, characterized by high extinction values ($>0.2\,\text{km}^{-1}$) and large
20 depolarization ($D > 10\%$), have been observed during the summer season, although not extending as far down in altitude as in Niger, but rather remaining confined between 1–5 km, still producing a tenfold increase in AOD.

The difference in the presence of aerosol in the lowermost layers (i.e. below 1 km) can be attributed to the fact that Banizoumbou is influenced by local dust sources (Rajot
25 et al., 2008).

A moderate background of dust aerosol with extinction values around 0.1 and depolarization greater then 10% is often present throughout the year in both sites.

The aerosol observed in M'Bour station in January and February show the presence of biomass burning, between 1.5 and 4 km. Occasionally, higher values of depolariza-

Variability of aerosol vertical distribution in the Sahel

O. Cavalieri et al.

tion in the uppermost layers shows the sporadic presence of dust aerosol.

In order to check the consistency of identification of aerosol typology based on observations, their occurrence is linked to the origin of airmasses sampled in measurement sites based on backtrajectories analysis arriving at the sites.

5   7 days back-trajectories are aggregated in cluster grouping arrival heights in three layers layers (0–2 km, 2–4 km, and 4–6 km) and are displayed in Figs. 2 and 3, together with ATSR fires for 2006, indicated by black crosses. Air mass backtrajectories have been marked by blue points.

During the dry season, air masses at low altitudes in Banizoumbou (Fig. 2) are mainly
10 coming from the Sahara desert and from the Atlantic region (upper left panel), while at higher levels (2–6 km) the air parcel are more confined in the Sahelian region matching most local biomass burning sources (upper central panel). This is somehow in partial contrast with the interpretation of the optical measurements given above, where biomass aerosol were more frequently in the lowermost levels.

15   Kim et al. (2009) focused observations of high concentrations of mineral dust aerosol from the surface to 1.5 or 2 km in Banizoumbou during January 2006 showing that dust is associated with airmass originating in the Saharan region, while at altitudes between 2–5 km, winds from the south or southeast brought biomass burning aerosol loaded airmasses from the source regions to the Sahel, in good accordance with the present
20 backtrajectory analysis.

It is possible that reduced time coverage during the dry season – profiles at the end of February – is mainly influenced by local sources that are not observed by ATSR and thus is poorly representative of average 2006 dry season condition. This point will be further discussed when presenting the CALIOP analysis.

25   During the summer season (from June to September) trajectories between 0 and 2 km of altitude (lower left panel) show two main pathways: monsoon circulation transport air from the Guinea Gulf, concurrently to a flow from North Africa related to the heat-low induced circulation. Both pathways are linked to observations which shows little or no presence of biomass aerosol. So, the analysis of 2006 lidar observations does

not provide any evidence of the cross equatorial transport of the extensive biomass burning occurring in the southern part of the continent at that time of the year highlighted by Real et al. (2010) and Barret et al. (2008) in the mid-troposphere.

Air masses at higher levels mainly come from the North, and North-East. In this period, the majority of observations are interpreted as DD, sometimes in very intense events, well in accordance with the transport pathways here discussed.

Trajectory analysis also shows that BBA which have been occasionally observed at our measurements sites, could probably originate from sparse fires in Northern Africa.

Backtrajectories arriving in Cinzana station shows a picture similar to Banizoumbou. During the dry season the air masses at low levels (up to 2 km of altitude) originates from Saharan desert in the North and from the Atlantic ocean (upper left panel) while between 2 and 6 km of altitude, the transport is mainly zonal, crossing biomass burning sources (upper central panel) in fair agreement with observations that shows the presence of BBA in layers between 2 and 5 km of altitude.

4 Inter-annual variability

The inter-annual pattern of aerosol variability over years 2006, 2007 and 2008 was studied by inspecting the AOD and Angstrom coefficient time series provided by the AERONET sunphotometers in the station of Banizoumbou, Cinzana and Dakar, and the total attenuated backscattering from the CALIOP lidar. For the sake of clarity, and for direct comparison with the ground based data, we have indicated these regions as M'Bour, Cinzana and, Banizoumbou for the westmost, central and eastmost region respectively. However, when comparing ground based with the satellite observations, it has to be borne in mind that the latter are in fact average values in the 11° N–15° N latitudinal band, grouped into longitudinal regions over, 15° W–20° W, 5° W–10° W and 0° E–5° E.

The profiles have been averaged over the 20 nearest CALIOP retrievals to the selected locations, which corresponds to an horizontal coverage of approximately 6.6 km.

Figures 4, 6 and 8 show respectively for Banizoumbou, Cinzana and M'Bour the 2006 (leftmost column), 2007 (central column) and 2008 (right column) time series of attenuated aerosol backscattering profiles (row a), AERONET AOD (row b) and Angstrom coefficient (row c).

⁵ A cloud mask has been applied to the CALIOP dataset to remove possible contribution from low level clouds, that appears in the plots as white zones where the data are absent.

As observed in all the three figures, the Sahelian region is characterized by a large day to day variability above all during summer season and this can be imputed to ¹⁰ scavenging processes during intense raining events.

4.1 Banizoumbou (11°–15° N; 0°–5° E)

A common seasonal pattern is discernible in Banizoumbou, in the total attenuated backscattering profiles (Fig. 5a) showing an aerosol burden starting at the lowermost levels – i.e. below 2 km – in January, slightly reducing in February then steadily increas- ¹⁵ ing from mid February to March. In that period, the aerosol burden at the lowermost levels is at its highest in 2007. The aerosol backscattering profile increases in verti- cal extension and intensity expanding up to 4–5 km of altitude in April and reaching the largest values between mid May and July when the monsoon activity induces a progressive clearing up of the atmosphere at the lowermost levels. At the end of the ²⁰ summer season the backscattering begin to taper off reducing its vertical extension and intensity until December, when it reaches the low winter values.

A clear seasonal pattern is evident in the AOD in Fig. 4b, showing larger values from January to September 0.5 and 2, with maxima up to 2.5–3 in intense events in spring (March–April) and in summer (June–July). Then it reduces to around 0.5 in the last ²⁵ part of the year. The interannual difference is limited. In the period January-February and June–July, the year 2007 shows larger AOD values with respect to the values in the other years.

The Angstrom coefficient is shown in Fig. 4c. It attains its higher values in the first

part of the year (in January–February, between 0.5 and 1) during July and August (up to 1.5) and in December (up to 1.5), often is correlated with low AOD values, indicating then the presence of smaller particles, which, according to the classification depicted in Table 1, can be attributed to the presence of BBA.

In the rest of the year, A stays below 0.5 in correspondence with large AOD values, indicating that dust particles, associated with the Saharan air masses, are then the dominant contributor to the AOD.

The limited interannual variability allows to evaluate the average seasonal evolution of aerosol based on CALIOP Depolarization and Color Index which have been used to identify different kind of aerosol. The joint probability density function (PDF) for D and Color Index observations for different seasons (column 1, January-February; column 2, March-April-May; column 3 June-July-August-September; column 4, November-December) and different atmospheric layers (on row a), the low layer between 0 and 2 km; on row b) the high layer between 2–6 km) is reported in Fig. 5. Each PDF is normalized for the number observations and is expressed in arbitrary units.

Observations with high D and low C are representative of DD aerosol while low D and high C are more representative of BBA. Intermediate optical characteristics are representative of mixed states.

For the dry season (JF in Fig. 5) a clear difference in particle optical properties is detectable between the low and the high layer. The most frequent observations in the elevated layer are for particles with typical optical values for BBA, while the lower layer has frequent observations of DD. Both DD and BBA shows a compact distribution in the D-C space showing, on a qualitatively basis that two layer appear to be well separated.

During MAM an increase of high D observations in the upper layer suggest an increasing presence of DD with lower values of PDF than in the lower layer. During the summer season (JJAS), DD observations are dominating in both layers, although a significant presence of BBA indicates clearly the observation of mixed states that are more pronounced in this season.

During fall (OND) DD observations are more probably than BBA in the lower layer

while the presence of BBA is predominant in the upper one.

4.2 Cinzana (11°–15° N, 5° W–10° W)

In Cinzana the seasonal pattern of the aerosol vertical distribution is similar to that observed in Banizoumbou. The CALIOP observations (Fig. 6a), show presence of aerosol up to 3 km of altitude at the beginning of the year (January–February), increasing in intensity and vertical extension up to 4–5 km at the beginning of the spring season, reaching maximum values in summer (June–July). The year 2008 is characterized by a large aerosol content below 2 km of altitude at the end of January and at middle February, with respect to 2007. A larger aerosol presence is also discernible at the end of 2006.

However, the bulk of the aerosol vertical distribution follows the same seasonal pattern observed over Banizoumbou. As for the Banizoumbou site, AOD values (Fig. 6b) are larger in the first part of the year (from January to September) compared to the end of the year with maximum values in spring and in summer.

In the period January–February and around mid July, the year 2007 is characterized by larger AOD values, between 0.5 and 1.5, with respect to the year 2006.

The Angstrom coefficient A (Fig. 6c) is greater than 0.5 in spring, markedly in April, in summer (from mid July to mid September) exceeding 1.5, while is reduced in the last part of the year, from the end of October to December, with values not exceeding 1.

Again these large values of A large are often in correspondence of low AOD values, suggesting the presence of BBA.

A slight year-to year difference is mainly confined to the dry season and summer onset: at the beginning of the year, 2006 is characterized by larger A values, up to 1 while in June–July the year 2007 shows A values up to 1.5. Figure 7 shows joint probability density function (PDF) for CALIOP D and Color Index observations over Cinzana. The difference of particle population between the layers is less evident with respect to Banizoumbou. The increase of high D observations in the upper layer of the atmosphere observed in MAM, indicative of an increasing presence of DD, is however

Title Page

Abstract | Introduction

Conclusions | References

Tables | Figures

◄ | ►►

◄ | ►

Back | Close

Full Screen / Esc

Printer-friendly Version

Interactive Discussion

still evident. During winter (JF) and fall (OND) the presence of DD is also observed in the upper layer respect with what happens in the other sites.

4.3 M'Bour (11°–15° N, 15° W–20° W)

Figure 9a reports the aerosol evolution over M'Bour showing clear annual evolution, analogously to Cinzana.

The bulk of the of aerosol vertical distribution is located around 3 km of altitude along all the year and its behaviour shows a less pronounced (with respect to Banizoumbou and Cinzana) seasonal variability of its vertical distribution with maxima in March and at mid July, when the AOD values goes up to 2.5.

The AOD values (Fig. 8b) are below 0.5 during the dry season and between end of October and December while AOD average values around 1 are present during the summer season and is generally lower than in the other two sites throughout the year.

The behaviour of A coefficient is also qualitatively similar to the inland sites with increased values during the winter and sporadic maxima during the summer season. Nevertheless, the intensity of A during BBA episodes during summer seems to be less pronounced than in Banizoumbou and Cinzana. Again the main features of the annual cycle are slightly variable year-to-year variation with the year 2006 characterized by larger A values during the dry season, suggesting more frequent observation of BBA.

Figure 9 shows joint probability density function (PDF) for CALIOP D and Color Index. The behaviour of PDF in the upper and lower layers closely resembles what observed in Banizoumbou. The clearly discernible difference of particle population between the high and low layers is still visible in winter (JF) and in fall (OND).

Finally, a noticeable presence of absorbing aerosol ($C < 0$) is observed in winter (JF) in the upper layers.

Title Page

Abstract | Introduction

Conclusions | References

Tables | Figures

◄◄ | ►►

◄ | ►

Back | Close

Full Screen / Esc

Printer-friendly Version

Interactive Discussion

4.4 Trajectory analysis

In order to evaluate the role of transport on the vertical and temporal variability of the aerosol discussed above, the number of back-trajectories encountering potential aerosol sources and ending in the three sites is estimated function of time and height.

Figure 10 reports the average position of airmasses 4 to 6 days before their arrival at Banizoumbou at 500 hPa, for the period January-February-March (JFM) 2006.

Trajectories are calculated on a daily basis at different pressure levels (as described in Sect. 2); in order to identify potential dust emissions, desert region is indicated with blue box while, in order to identify air masses transported from Monsoon flow Guinea Gulf area is enclosed in the yellow box.

Red solid contour encompasses the regions where forest fires, as observed from AATSR, occurred..

The superposition of the trajectories the BBA sources indicates that in winter at the 500 hPa level airmasses came preferentially from region of BBA emission, rather than from desert region and northward transport from Equatorial Africa is inhibited by the winter circulation (Fig. 11a).

Such plots have also been produced also for Cinzana and M'Bour for all seasons and all years, and are available in the supplementary material associated with this article.

Figure 12 summarizes the variability of backtrajectories, showing the time-height evolution of airmasses encountering the Desert region (blue) transported by the Monsoon flow (yellow) and encountering Biomass burning (red) for three sites (columns a to c) and 2006–2008 years (rows a to c).

A remarkably similar pattern of airmasses origins is present throughout the three years study, and in common to the three sites.

Air from the Saharan desert is present throughout the year. It is observed in the lower layers in the first and last part of the year, and extending upward in the central part of the year. At that time, the lower layers result to be less affected by influence from the Sahara when the monsoon flow carries in land air from the Guinea Gulf and

the Southern Hemisphere. Biomass burning influence is mainly confined in the higher layers, observable at the beginning and at the end of the year, although sparse events might still be discerned throughout the year. Noteworthy, the desert influence is remarkably similar in the three sites for the second part of the year, while during spring, it decreases westward from Banizoumbou to M'Bour.

Figure 11 does not show a large inter-annual variability of the air masses circulation over the three sites; the main differences are observed over Cinzana site in summer 2007 when the monsoon flow from the Guinea Gulf is almost absent in the lower layers of the atmosphere if compared to the other years, and during the dry season 2008 over both Banizoumbou and Cinzana sites when the layers above 3 km of altitude are less affected by air masses influenced by biomass burning.

The seasonal pattern of air mass influences and the main difference in the air mass circulation are confirmed by AOD and A time series analysis shown in Figs. 4, 6 and 8 for the three sites over the three years and discussed here above.

5   Summary and conclusions

In this work, we have studied the seasonal and inter-annual variability of the aerosol vertical distribution over three years in the Sahel region, characterizing the different kind of aerosols present in the atmosphere in terms of their optical properties observed by ground-based and satellite instruments, and their sources searched for by using trajectory studies.

During winter, the lower levels air masses arriving in the Sahelian region come mainly from North, North-West and from the Atlantic area, while in the upper troposphere air flow generally originates from West Africa, crossing a region characterized by the presence of large biomass burning sources. The sites of Cinzana, Banizoumbou and M'Bour, along a transect of aerosol transport from East to West, are in fact under the influence of tropical biomass burning aerosol emission during the dry season, as revealed by the seasonal pattern of the aerosol optical properties, and by backtrajectory

Variability of aerosol vertical distribution in the Sahel

O. Cavalieri et al.

studies. There, BBA are mainly observed in January–February, confined in the upper layers of the atmosphere. This is particularly evident for year 2006, which was characterized by a large presence of biomass burning aerosols in all the three sites.

Biomass burning influenced aerosols are also observed in the summer season (from July to September) transported by the monsoon flow coming from the south Africa region characterized by the presence of large biomass burning sources.

Sporadic biomass burning events are also observed in spring, since in this period air masses coming from North Africa and Saharan desert pass on sparse biomass burning sources placed in the tropical area.

During summer months, the entire Sahelian area is under the influence of Saharan dust aerosols: the air masses in low levels arrived or from West Africa crossing the Saharan desert or from the Southern Hemisphere crossing the Guinea Gulf while in the upper layers air masses still originated from North, North-East. The maximum of the desert dust activity is observed in this period, widespread along the entire Sahelian transect, characterized by large AOD and backscattering values. It also corresponds to a maximum in the extension of the aerosol vertical distribution (up to 6 km of altitude). In correspondence, a progressive cleaning up of the lowermost layers of the atmosphere is occurring, especially evident in Banizoumbou and Cinzana sites.

Summer is in fact characterized by extensive and fast convective phenomena.

Lidar profiles shows at times large dust events loading the atmosphere with aerosol from the ground up to 6 km of altitude. These events are characterized by large total attenuated backscattering values, and alternate with very clear profiles, sometimes separated by only a few hours, indicative of fast removal processes occurring, likely due to intense convective and rain activity.

This work has provided a long-term characterization of Sahelian aerosol from seasonal to multiannual timescale. Different kind of aerosol have been defined according to their optical characteristics, their seasonal evolution has been tracked during three years, and their sources have been searched for with the aid of trajectory studies,

whose outcome showed good accordance with what inferred from the observations.

Supplementary material related to this article is available online at:
http://www.atmos-chem-phys-discuss.net/10/17609/2010/
acpd-10-17609-2010-supplement.pdf.

References

Alpert, P., Neeman, B. U., and Shay-el, Y.: Climatological analysis of Mediterranean cyclones using ECMWF data, Tellus, 42A, 65–77, 1990.

Angstrom, A.: The parameters of atmospheric turbidity, Tellus, 16, 64–75, 1964.

Ansmann, A., Bsenberg, J., Chaikovsky, A., Comeron, A., Eckhardt, S., Eixman, R., Freudenthaler, V., Ginoux, P., Komguem, L., Linn, H., Lopez Marquea, M.A., Matthis, V., Matthis,

Variability of aerosol vertical distribution in the Sahel

O. Cavalieri et al.

I., Mitev, V., Mller, D., Music, S., Nickovic, S., Pelon, J., Sauvage, L., Sobolewsky, P., Srivastava, M., and Wiegner M.: Long range transport of Saharan dust to north-ern Europe: The 11–16 October 2001 ourtbreak observed with EARLINET, J. Geophys. Res., 108, 4783, doi:101029/2003JD003757, 2003.

5   Balis, D. S., Amiridis, V., Nickovic, S., Papayannis, A., and Zerefos, C.: Optical properties of Saharan dust layers as detected by a Raman lidar at Thessaloniki, Greece, Geophys. Res. Lett., 31, L13104, doi:10.1029/2004GL019881.c, 2004.

Barret, B., Ricaud, P., Mari, C., Attié, J.-L., Bousserez, N., Josse, B., Le Flochmoën, E., Livesey, N. J., Massart, S., Peuch, V.-H., Piacentini, A., Sauvage, B., Thouret, V., and Cammas, J.-P.:
10   Transport pathways of CO in the African upper troposphere during the monsoon season: a study based upon the assimilation of spaceborne observations, Atmos. Chem. Phys., 8, 3231–3246, doi:10.5194/acp-8-3231-2008, 2008.

Cattrall, A., Reagan, J., Thome, K., and Dubovik, O.: Variability of aerosol and spectral lidar and backscatter and extinction ratios of key aerosol types derived from selected Aerosol Robotic
15   Network locations, J. Geophys. Res.,110, D10S11, doi:10.1029/2004JD005124, 2005.

Cavalieri, O., Di Donfrancesco, G., Cairo, F., Fierli, F., Snels, M., Viterbini, M., Cardillo, F., Chatenet, B., Formenti, P., Marticorena, B., and Rajot, J. L.: The AMMA mulid network for aerosol characterization in West Africa, Int. J. of Remote Sens., in press, 2010.

Dayan, U., Heffter, J., Miller, J., and Gutman, G.: Dust intrusion events into the Mediterranean
20   basin, J. Appl. Meteorol., 30, 1185–1198, 1991.

De Tomasi, F., Blanco, A., and Perrone, M. R.: Raman lidar monitoring of extinction and backscattering of African dust layers and dust characterization, Appl. Optics, 42(9), 1699–1709, 2003.

Ferrare, R. A., Turner, D. D., Brasseur, L. H., Feltz, W. F., Dubovik, O., and Tooman, T. P.:
25   Raman lidar measurements of the aerosol extinction to backscatter ratio over the Southern Great Plains, J. Geophys. Res., 106, 20333–20347, 2001.

Fiebig, M., Petzold, A., Wandinger, U., Wendisch, M., Kiemle, C., Stifter, A., Ebert, M., Rother, T., and Leiterer, U.: Optical closure for an aerosol column: method, accuracy, and inferable properties applied to a biomass-burning aerosol and its radiative forcing, J. Geophys. Res.,
30   107, 8130, doi:10.1029/2000JD000192, 2002.

Devara, P. C. S., Pandithurai, G., Raj, P. E., and Sharma, S.: Investigations of aerosol optical depth variations using spectroradiometer at an urban station. Oune, India, J. Aerosol Sci., 27, 621–632, 1996.

Variability of aerosol vertical distribution in the Sahel

O. Cavalieri et al.

Title Page

Abstract | Introduction

Conclusions | References

Tables | Figures

|◄ | ►|

◄ | ►

Back | Close

Full Screen / Esc

Printer-friendly Version

Interactive Discussion

Di Donfrancesco, G., Cairo, F., Buontempo, C., Adriani, A., Viterbini, M., Snels, M., Morbidini, R., Piccolo, F., Cardillo, F., Pommereau, J. P., and Garnier, A.: Balloonborne Lidar for cloud physics studies, Appl. Optics, 42(22), 5701–5708, 2006.

Di Sarra, A., Di Iorio, T., Cacciani, M., Fiocco, G., and Fuà, D.: Saharan dust profiles measured by lidar at Lampedusa, J. Geophys. Res., 106(D10), 335–347, 2001.

Dubovik, O. and King, M. D.: A flexible inversion algorithm for retrieval of aerosol optical properties from Sun and sky radiance measurements, J. Geophys. Res., 105, 20673–20696, 2002.

Dubovik, O., Smirnov, A., Holben, B. N., King, M. D., Kaufman, Y. J., Eck, T. F., and Slutsker, I.: Accuracy assessments of aerosol optical properties retrieved from Aerosol Robotic Network (AERONET) Sun and Sky radiance measurements, J. Geophys. Res., 105(D8), 9791–9806, 2000.

Eck, T. F., Holben, B. N., Ward, D. E., Mukelabai, M. M., Dubovik, O., Smirnov, A., Schafer, J. S., Hsu, N. C., Piketh, S. J., Queface, A., Le Roux, J., Swap, R. J., and Slutsker, I.: Variability of biomass burning aerosol optical characteristics in southern Africa during the SAFARI 2000 dry season campaign and a comparison of single scattering albedos estimates from radiometric measurements, J. Geophy. Res., 108(D13), 8477, doi:10.1029/2002JD002321, 2003.

Forster, P., Ramaswamy, V., Artaxo, P., Berntsen, T., Betts, R., Fahey, D. W., Haywood, J., Lean, J., Lowe, D. C., Myhre, G., Nganga, J., Prinn, R., Raga, G., Schulz, M., and Van Dorland, R.: Changes in atmospheric constituents and in radiative forcing in Climate Change 2007: The Physical Science Basis. Contribution of Working Group I to the Fourth Assesment Report of the Intergovernmental Panel on Climate Change, edited by: Solomon, S., Quin, D., Manning, M., et al., Cambridge Univ. Press, Cambridge, UK, 129–234, 2007.

Gobbi, G. P., Barnaba, F., Giorgi, R., and Santacasa, A.: Altitude-resolved properties of a Saharan dust event over Mediterranean, Atmos. Environ., 34, 5119–5127, 2000.

Hamonou, E., Chazette, P., Balis, D., Dulac, F., Schneider, X., Galani, E., Ancellet, G., and Papayannis, A.: Characterization of the vertical structure of Saharan dust export to the Mediterranean basin, J. Geophys. Res., 22257–22270, 1999.

Haywood, J. M., and Boucher, O.: Estimates of the direct and indirect aerosols: a review, Rev. Geophys., 38, 513–543, 2000.

Haywood, J., Francis, J., Osborne, S., Glew, M., Loeb, N., Highwood, E., Tanrè, D., Myhre, G., Formenti, P., and Hirst, E.: Radiative properties and direct radiative effect of Saharan

Variability of aerosol vertical distribution in the Sahel

O. Cavalieri et al.

Title Page

Abstract | Introduction

Conclusions | References

Tables | Figures

◄ | ►

◄ | ►

Back | Close

Full Screen / Esc

Printer-friendly Version

Interactive Discussion

dust measured by the C-130 aircraft during SHADE: 1. Solar spectrum, J. Geophy. Res., 108(D18), 8577, doi:10.1029/2002JD002687, 2003.

Haywood, J. M., Pelon, J., Formenti, P., Bharmal, N., Brooks, M., Capes, G., Chazette, P., Chou., C., Christopher, S., Coe, H., Cuesta, J., Derimian, Y., Desboeufs, K., Greed, G., Harrison, M., Heese, B., Highwood, E. J., Johnson, B., Mallet, M., Marticorena, B., Marsham, J., Milton, S., Myhre, G., Osborne, S. R., Parker, D. J., Rajot, J. L., Schulz, M., Silingo, A., Tanrè, D., and Tulet, P.: Overview of the Dust and Biomass-burning Experiment and African Monsoon Multidisciplinary Analysis Special Observing Period-0, J. of Geoph. Res., 113, D00C17, doi:10.1029/2008JD010077, 2008.

Heese, B. and Wiegner, M.: Vertical aerosol profiles from Raman-depolarization lidar observations during the dry season AMMA field campaign, J. Geophys. Res., 113, D00C11, doi:10.1029/2007JD009487, 2008.

Immler, F. and Schrems, O.: Vertical profiles, optical and microphysical properties of Saharan dust layers determined by a ship-borne lidar, Atmos. Chem. Phys., 3, 1353–1364, doi:10.5194/acp-3-1353-2003, 2003.

Johnson, B., Osborne, S., Haywood, J., and Harisson, M.: Aircraft measurements of biomass burning aerosol over West Africa during DABEX, J. Geophys. Res., 113, D00C06, doi:10.1029/2007JD009451, 2008.

Junge, C. E.: Air chemistry and radioactivity. Academic Press Inc., New York, 1963.

Leon, J. F., Derimian, Y., Chiapello, I., Tanrè, D., Podvin, T., Chatenet, B., Diallo, A., and Deroo, C.: Aerosol vertical distribution and optical properties over M'Bour (16.96° W; 14.39° N), Senegal from 2006 to 2008, 2009.

Liu, L. and Mishchenko, I.: Constraints on PSC particle microphysics derived from lidar observations, J. Quant. Spectrosc. Ra., 70, 817–831, 2001.

Kim, S.-W., Chazette, P., Dulac, F., Sanak, J., Johnson, B., and Yoon, S.-C.: Vertical structure of aerosols and water vapor over West Africa during the African monsoon dry season, Atmos. Chem. Phys., 9, 8017–8038, doi:10.5194/acp-9-8017-2009, 2009.

Magi, A., Hobbs, P. V., Schmid, B., and Redemann, J.: Vertical profiles of light scattering, light absorption and single-scattering albedo during the dry, biomass burning season in southern Africa and comparisons of in situ and remote sensing measurements of aerosol optical depths, J. Geophys. Res., 108(D13), 8504, doi:10.1029/2002JD002361, 2003.

Marticorena, B. and Bergametti, G.: Two-year simulations of the seasonal and interannual changes of the Saharan dust emissions, Geophys. Res. Lett., 23(15), 1921–1924, 1996.

Variability of aerosol vertical distribution in the Sahel

O. Cavalieri et al.

Title Page

Abstract	Introduction
Conclusions	References
Tables	Figures

|◄ | ►|

◄ | ►

Back | Close

Full Screen / Esc

Printer-friendly Version

Interactive Discussion

Mattis, I., Ansmann, A., Muller, D., Wandinger, U., and Althausen, D.: Dual-wavelenght Raman lidar observations of the extinction-to backscatter ratio of Saharan dust, Geophys. Res. Lett., 29(9), 1306, doi:10.1029/2002GL014721, 2002.

Mishcenko, M. I., Kahn, R. A., and West, R. A.: Modeling phase functions for dustlike tropospheric aerosols using a shape mixture of randomly oriented polydisperse spheroids, J. Geophys. Res., 102(D14), 831–847, 1997.

Mona, L., Amodeo, A., Pandolfi, M., and Pappalardo, G.: Saharan dust intrusions in the Mediterranean area: Three years of Raman lidar measurements, J. Geophys. Res., 111(D16), D16203.1–D16203.13, doi:10.1029/2005JD006569, 2006.

Moulin, C., Lambert, C., Dulac, F., and Dayan, U.: Control of atmospheric export of dust from North Africa by the North Atlantic Oscillation, Nature, 387, 691–694, 1997.

Osborne, S., Johnson, B., Haywood, J., Baran A., Harrison, M., and McConnell, C.: Physical and optical properties of mineral dust aerosol during the Dust and Biomass-burning Experiment, J. Geophys.Res., 113, D00C03, doi:10.1029/2007JD009551, 2008.

Pelon, J., Mallet, M., Mariscal, A., Goloub, P., Tanrè, D., Bou Karam, D., Flamant, C., Haywood, J., Pospichal, B., and Victori, S.: Microlidar observations of biomass burning aerosol over Djougou (Benin) during African Monsoon Multidisciplinary Analysis Special Observation Period 0: Dust and Biomass Burning Experiment, J. Geophys. Res., 113, D00C18, doi:10.1029/2008JD009976, 2008.

Prospero, J. M., Ginoux, P., Torres, O., Nicholson, S. E., and Gill, T. E.: Environmental characterization of global sources of atmospheric soil dust identified with the Nimbus 7 total ozone mapping spectrometer (TOMS) absorbing aerosol product, Rev. Geophys., 40(1), 1002, doi:10.1029/2000RG000095, 2002.

Prospero, J. M. and Carlson, T. N.: Vertical and areal distribution of Saharan dust over the western equatorial North Atlantic Ocean, J. Geophys. Res., 77, 5255–5265, 1972.

Rajot, J. L.: Wind blown sediment mass budget of Sahelian village land units in Niger", Bulletin de la Societe Géologique de France, 172(5), 523–531, 2001.

Rajot, J. L., Alfaro, S., Desboeufs K., Chevaillier, S., Formenti, P., Triquet, S., Chatenet, B., Gaudichet, A., Journets, E., Maman, A., Mouget, N., and Zakou, A.: AMMA dust experiment: An overview of measurements performed during the dry season special observation period (SOP0) at the Banizoumbou (Niger) supersite, J. Geophys. Res., 113, D00C14, doi:10.1029/2008JD009906, 2008.

Raut, J.-C and Chazette, P.: Radiative budget in the presence of multi-layered aerosol

Title Page

Abstract | Introduction

Conclusions | References

Tables | Figures

◄ | ►►

◄ | ►

Back | Close

Full Screen / Esc

Printer-friendly Version

Interactive Discussion

structures in the framework of AMMA SOP-0, Atmos. Chem. Phys., 8, 6839–6864, doi:10.5194/acp-8-6839-2008, 2008.

Reagan, J. A., McCormick, M. P, and Spinhirne, J. D.: Lidar sensing of aerosols and clouds in the troposphere and stratosphere, Proceedings of the IEEE, 77(3), SSN 0018-9219, doi:10.1109/5.24129 1989.

Real, E., Orlandi, E., Law, K. S., Fierli, F., Josset, D., Cairo, F., Schlager, H., Borrmann, S., Kunkel, D., Volk, C. M., McQuaid, J. B., Stewart, D. J., Lee, J., Lewis, A. C., Hopkins, J. R., Ravegnani, F., Ulanovski, A., and Liousse, C.: Cross-hemispheric transport of central African biomass burning pollutants: implications for downwind ozone production, Atmos. Chem. Phys., 10, 3027–3046, doi:10.5194/acp-10-3027-2010, 2010.

Redelsperger, J. L., Thorncroft, C. D., Diedhiou, A., Lebel, T., Parker, D. J., and Polcher, J.: African Monsoon Multidisciplinary Analysis. An International Research Project and Field Campaign, B. Am. Meteorol. Soc, 87(12), 1739–1746, 2006.

Schmid, B., Redemann, J., Russell, P. B., Hobbs, P. V., Hlavka, D. L., McGill, M. J., Holben, B. N., Welton, E. J., Campbell, J. R., Torres, O., Kahn, R. A., Diner, D. J., Helmlinger, M. C., Tanré, D., Haywood, J. M., Pelon, J., Lon, J. F., Chatenet, B., Formenti, P., Francis, P., Goloub, P., Highwood, E. J., and Myhre, G.: Measurement and modeling of the Saharan dust radiative impact: overview of the SaHAran Dust Experiment (SHADE), J. Geophys. Res., 108(D13), 8574, doi:10.1029/2002JD003273, 2003.

Swap, R., Garstang, M., Greco, S., Talbot, R., and Kallberg, P.: Saharan dust in the Amazon Basin, Tellus, 44B, 133–149, 1992.

Swap, R. J., Annegarn, H. J., Suttles, J. T., King, M. D., Platnick, S., Privette, J. L., and Scholes, R. J.: Africa burning: A thematic analysis of the Southern African Regional Science Initiative (SAFARI 2000), J. Geophys. Res., 108(D13), 8465, doi:10.1029/2003JD003747, 2003.

Tafuro A. M., Barnaba F., and De Tomasi, F.: Saharan dust particle properties over the central Mediterranean, Atmos. Res., 81, 67–93, 2006.

Tanrè, D., Haywood, J., Pelon, J., L'eon, J.-F., Chatenet, B., Formenti, P., Francis, P., Goloub, P., Highwood, E., and Myhre, G.: Measurement and modeling of the Saharan dust radiative impact: Overview of the Saharan Dust Experiment (SHADE), J. Geophys. Res., 108, 8574, doi:10.1029/20023273, 2003.

Wandinger, U., Mller, D., Bckmann, C., Althausen, D., Matthias, V., Bsenberg, J., Wei, V., Fiebig, M., Wendisch, M., Stohl, A., and Ansmann, A.: Optical and microphysical characterization of biomass-burning and industrial-pollution aerosols from multi wavelength lidar and aircraft

Variability of aerosol vertical distribution in the Sahel

O. Cavalieri et al.

Title Page

Abstract	Introduction
Conclusions	References
Tables	Figures

I◄ ►I

◄ ►

Back Close

Full Screen / Esc

Printer-friendly Version

Interactive Discussion

measurements, J. Geophys. Res., 107(D21), 8125, doi:10.1029/2000JD000202, 2002.

Winker, D. M., Hunt, W. H, and McGill, M. J.: Initial performance assessment of CALIOP, Geophys. Res. Lett., 34, L19803, doi:10.1029/2007GL030135, 2007.

Variability of aerosol vertical distribution in the Sahel

O. Cavalieri et al.

Title Page

Abstract	Introduction
Conclusions	References
Tables	Figures

◄◄   ►►

◄   ►

Back   Close

Full Screen / Esc

Printer-friendly Version

Interactive Discussion

Table 1. Classification of desert dust and biomass burning aerosol depending on Volume Depolarization Ratio (D), Color Index (C) and Angstrom coefficient (A) values.

Type of Aerosol	D (%)	C	A
Desert Dust	$> 10\%$	< 0.5	~ 0
Biomass Burning	$< 10\%$	> 0.5 up to 3	1.–1.5

Table 2. Mulid System Parameters.

Parameter	Value
Wavelengths	1064 nm and 532 nm
Laser Type	Nd: YAG
Pulse duration	10 ns
Laser repetition rate	0.3 Hz
Laser output energy	10 mJ at 1064 nm
	5 mJ at 532 nm
Telescope diameter	20 cm
Telescope type	Newtonian f/1.5
Telescope field of view	0.666 mrad
Beam divergence	0.5 mrad, full angle
	×4 expanded
Effective Filter bandwidth	2 nm
Raw data resolution	30 m photo-counting
	3.75 m analog mode
Processed data resolution	30 m

Full Screen / Esc

Printer-friendly Version

Interactive Discussion
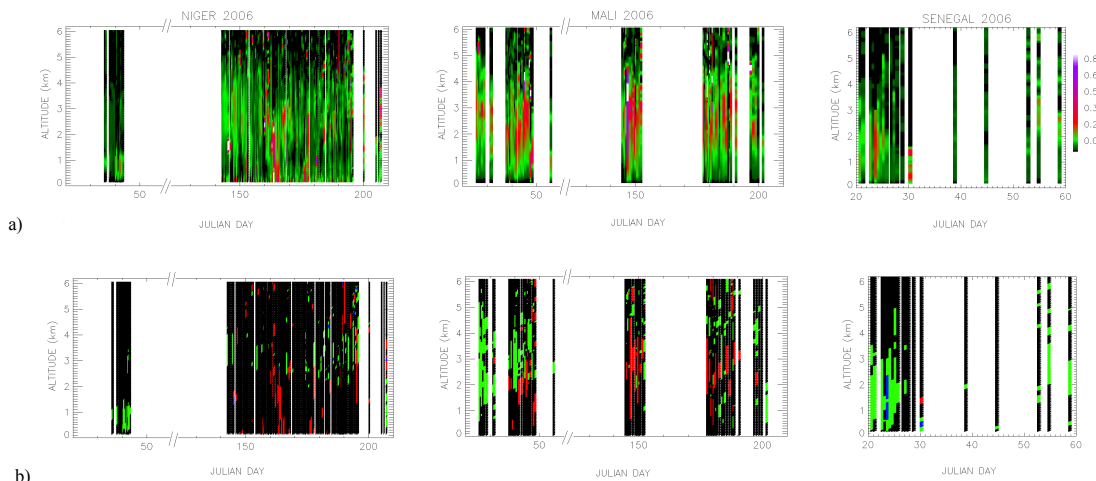
Fig. 1. In the upper panels are shown **(a)** 144 extinction profiles from February to August 2006 from the Niger MULID (left), 48 extinction profiles from January to July 2006 from the Mali MULID (middle) and 19 extinction profiles from the Senegal MULID site (right) and below **(b)** are pointed out, in each extinction profile, the different kind of aerosol observed on Banizoumbou (left), Cinzana (middle) and M'Bour stations (right) by MULID systems during year 2006: intense DD events (red), BBA (green) and the mixing between dust and biomass burning aerosols (blue). The "background" aerosol burden is in black. In panel **(c)** are shown top, bottom and barycentre (x) of vertical distribution for Banizoumbou (left), Cinzana (middle) and M'Bour (right) sites and finally panel **(d)** presents AOD values for Banizoumbou (left), Cinzana (middle) and M'Bour (right) stations.
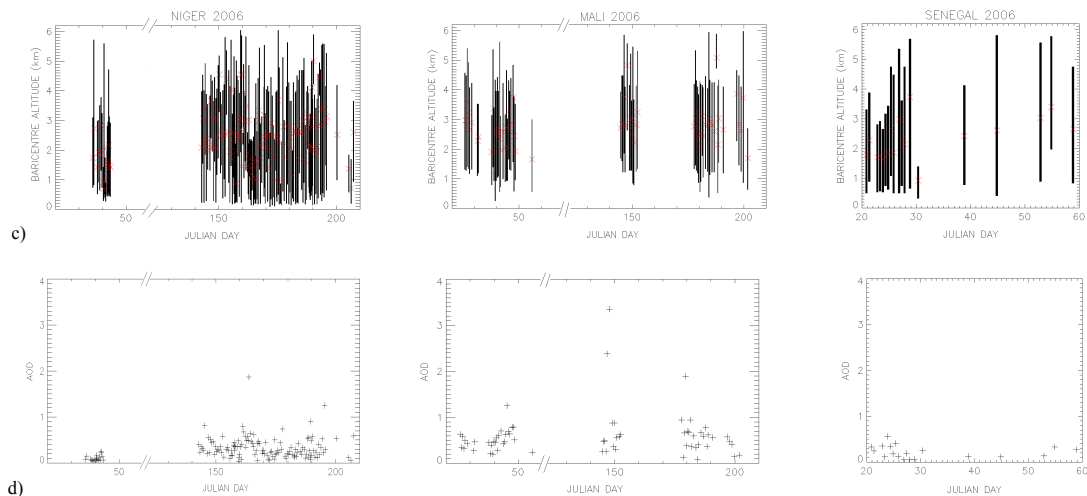
Fig. 1. Continued.

Variability of aerosol vertical distribution in the Sahel

O. Cavalieri et al.
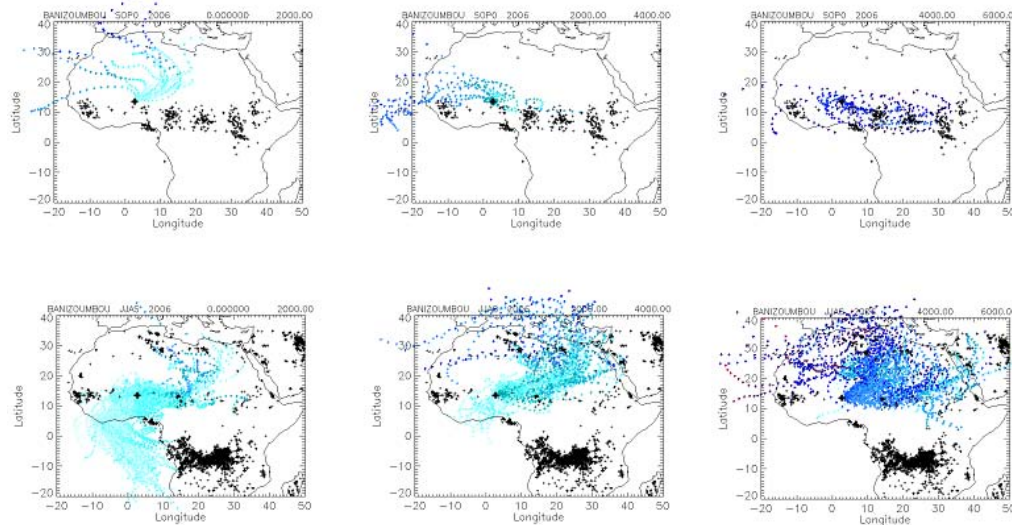
Fig. 2. Aeronet 7 day back trajectories ending on Banizoumbou site between 0–2 km (left), 2–4 km (middle), 4–6 km (right) and biomass burning emission map (black +) for the period January–February 2006 (upper panel) and June–September 2006 (lower panel).

Full Screen / Esc

Printer-friendly Version

Interactive Discussion
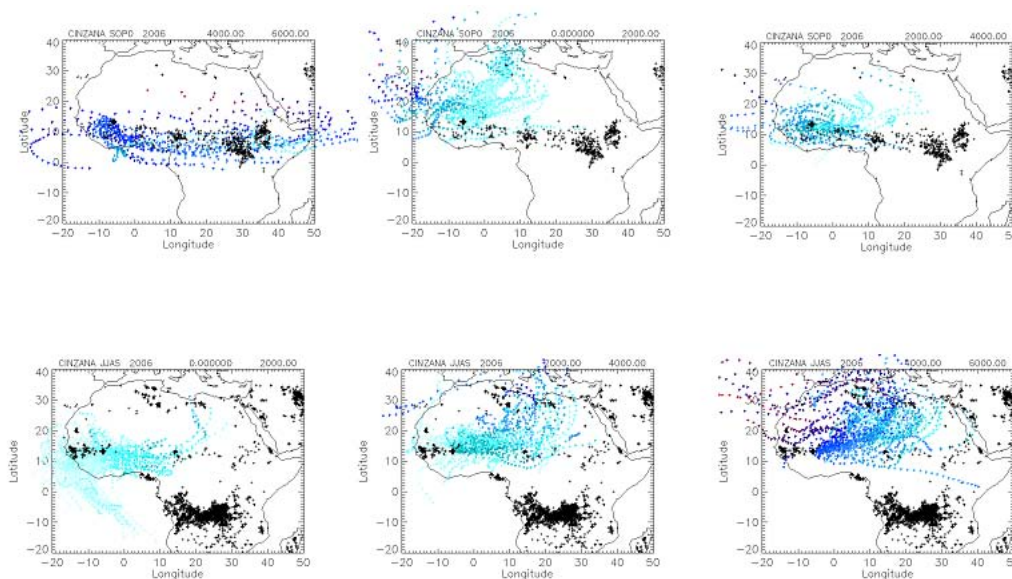
Fig. 3. Aeronet 7 day back trajectories ending on Cinzana site between 0–2 km (left), 2–4 km (middle), 4–6 km (right) and biomass burning emission map (black +) for the period January–February 2006 and June–September 2006 (lower).
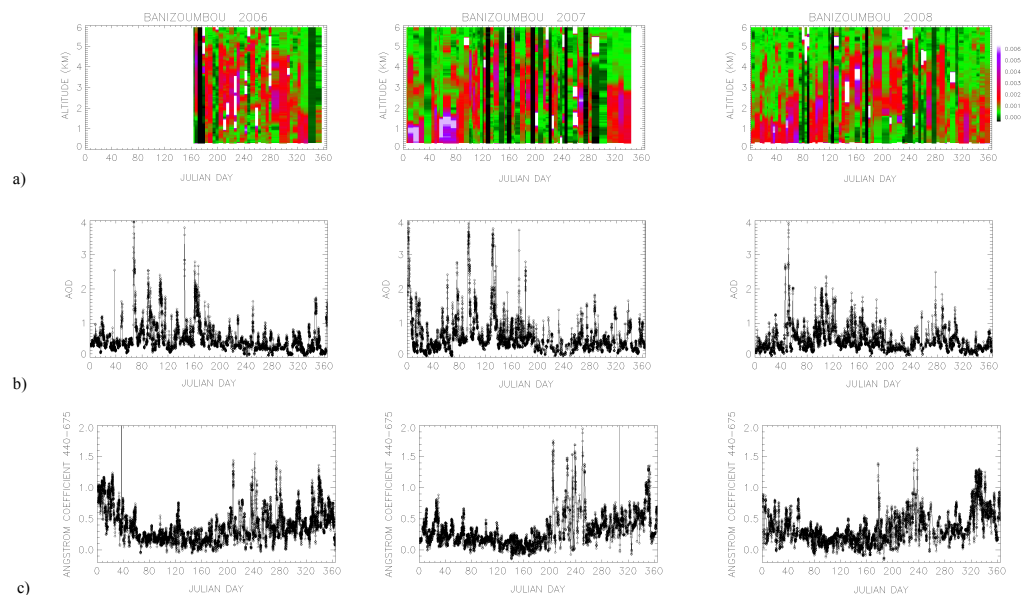
Fig. 4. Total attenuated backscatter (km^{-1} sr^{-1}) profiles from Calipso database **(a)**, AOD **(b)** and Angstrom coefficient **(c)** time series estimated at 532 nm from AERONET database for year 2006 (left), 2007 (middle) and 2008 (right) at Banizoumbou site.
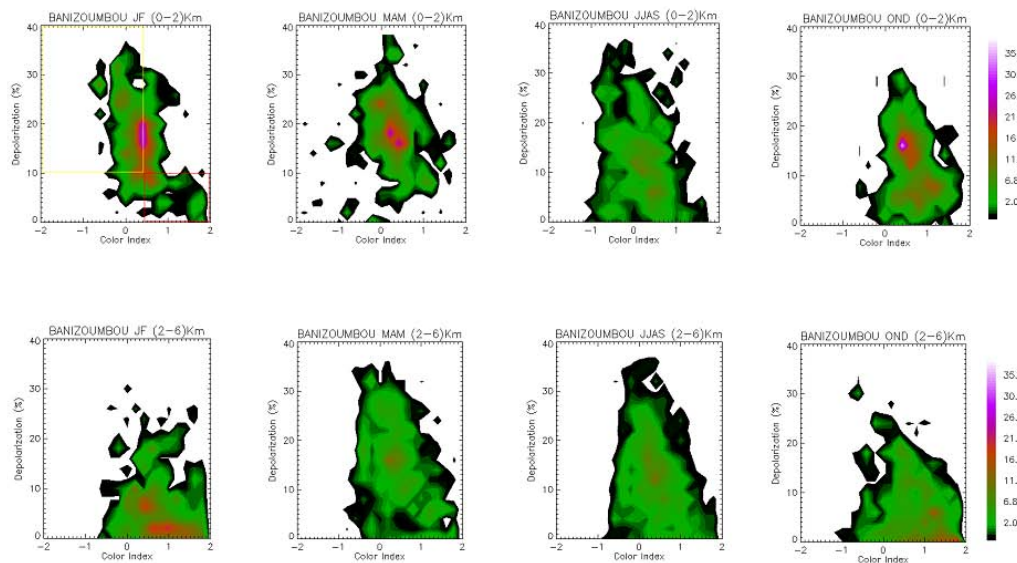
Fig. 5. Joint PDF for Color Index and Depolarization Caliop observations for different seasons (column 1, January–February; column 2, MAM; column 3, JJAS; column 4, OND) and different atmospheric layers (row **(a)** 0–2 km; **(b)** 2–6 km) for Banizoumbou site. In the upper left panel the yellow and red rectangles identify, respectively, desert dust and biomass burning aerosols classified using color index and depolarization values as depicted in Table 1. Colored rectangles are shown only in one panel for safety of clarity.
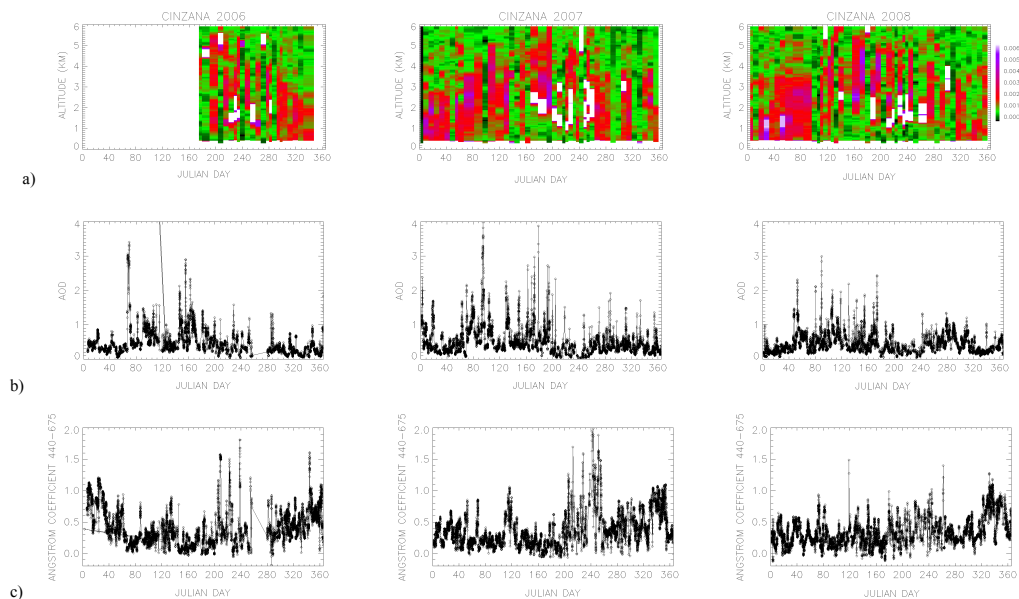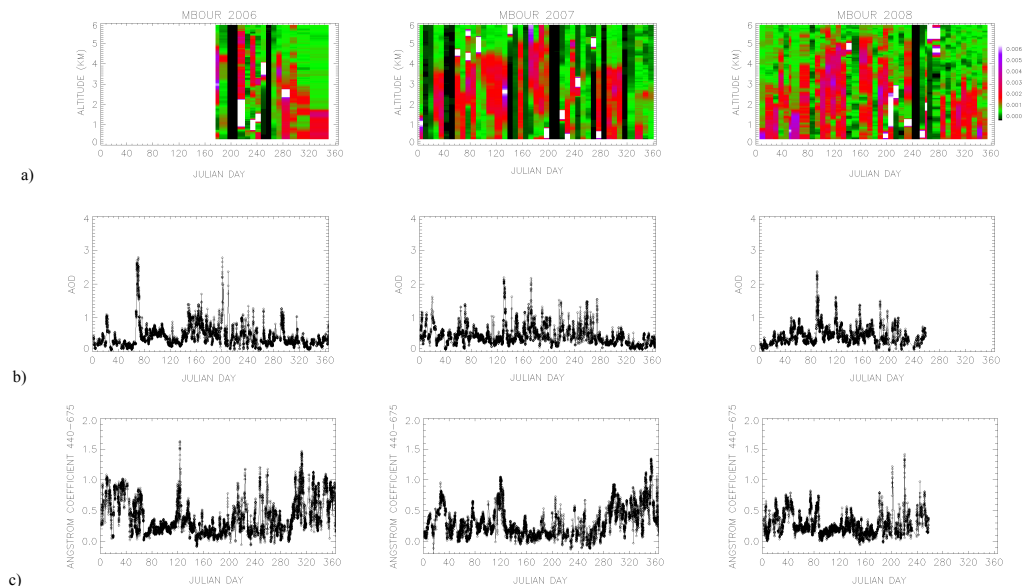
Fig. 6. Total attenuated backscatter ($km^{-1} sr^{-1}$) profiles from Calipso database **(a)**, AOD **(b)** and Angstrom coefficient **(c)** time series estimated at 532 nm from AERONET database for year 2006 (left), 2007 (middle) and 2008 (right) at Cinzana site.
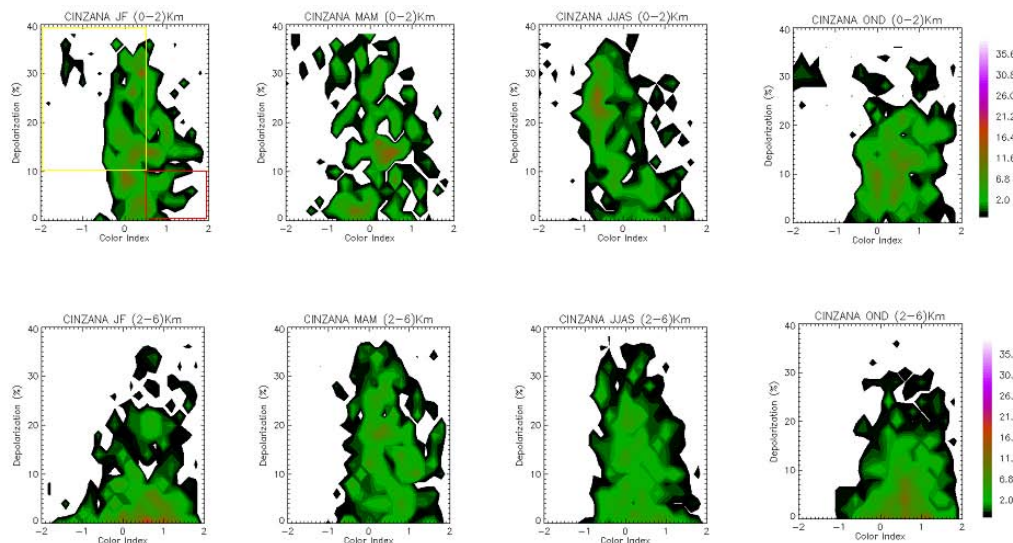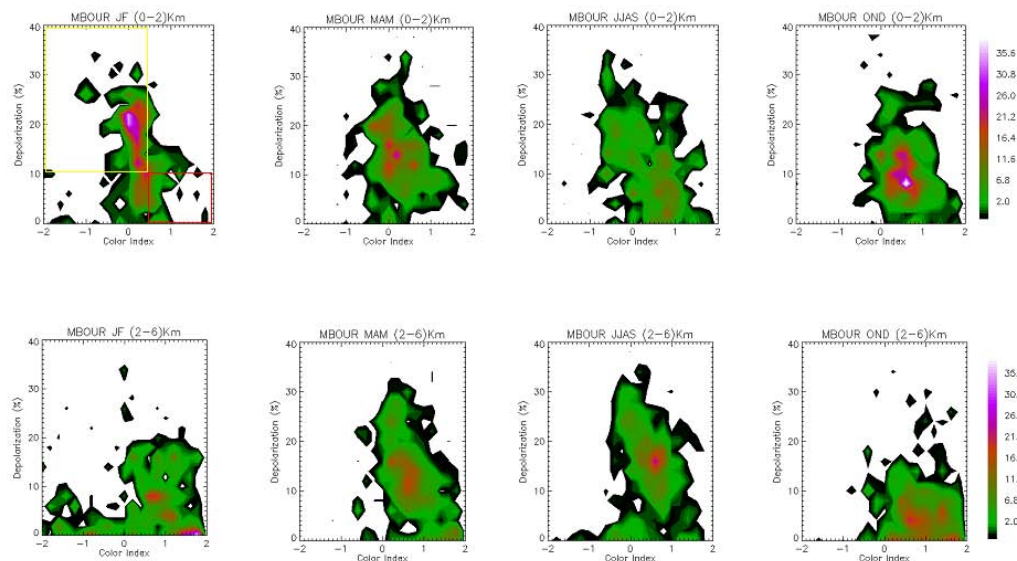
Fig. 7. Joint PDF for Color Index and Depolarization Caliop observations for different seasons (colum 1, JF; column 2, MAM; column 3, JJAS; column 4, OND) and different atmospheric layers (row **a**) 0–2 km; **b**) 2–6 km) for Cinzana site. In the upper left panel the yellow and red rectangles identify, respectively, desert dust and biomass burning aerosols classified using color index and depolarization values as depicted in Table 1. Colored rectangles are shown only in one panel for safety of clarity.

Fig. 8. Total attenuated backscatter (km^{-1} sr^{-1}) profiles from Calipso database **(a)**, AOD **(b)** and Angstrom coefficient **(c)** time series estimated at 532 nm from AERONET database for year 2006 (left), 2007 (middle) and 2008 (right) at Dakar site.

Title Page

Abstract | Introduction

Conclusions | References

Tables | Figures

◄◄ | ►►

◄ | ►

Back | Close

Full Screen / Esc

Printer-friendly Version

Interactive Discussion

Fig. 9. Joint PDF for Color Index and Depolarization Caliop observations for different seasons (colum 1, JF; column 2, MAM; column 3, JJAS; column 4, OND) and different atmospheric layers (row **a**) 0–2 km; **b**) 2–6 km) for M'Bour site. In the upper left panel the yellow and red rectangles identify, respectively, desert dust and biomass burning aerosols classified using color index and depolarization values as depicted in Table 1. Colored rectangles are shown only in one panel for safety of clarity.
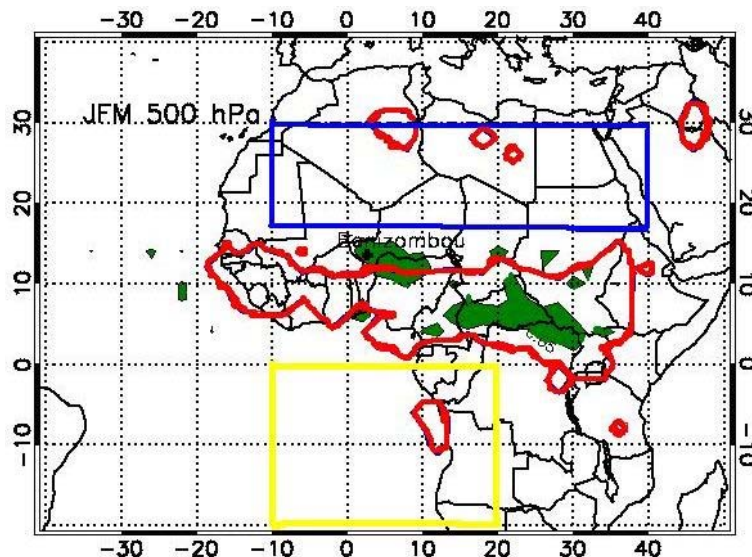
Fig. 10. Number of trajectories per day averaged in January-February-March (JFM) 2006. Trajectories are binned in a 2° latitude-longitude grid. Green contours represent the average position 4 to 6 days before arrival at 500 hPa over Banizoumbou. Red contours indicates areas where forest fires observed from AATSR occurs. Fire-pixel are taken into account if their number is larger than 10 in the three-months period. Areas defined as "Desert" and "Ocean" are indicated by blue and yellow rectangles respectively.
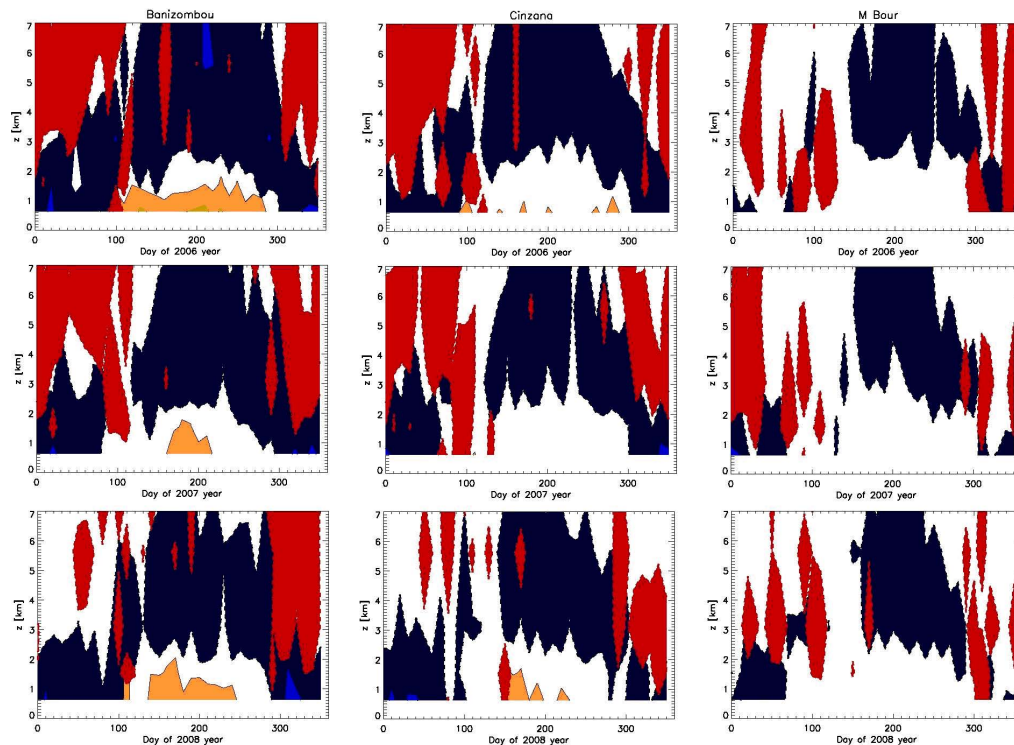
Fig. 11. Time-height evolution for airmasses coming from "Desert" region (blue) and "Ocean" (yellow) and encountering Forest fires observed by AATSR (Red). Number of trajectories is averaged on ten days. Units are arbitrary.